Published in final edited form as:
ACS Appl Mater Interfaces. 2013 June 12; 5(11): 4904–4912. doi:10.1021/am4006397.

Nitric Oxide-Releasing Xerogels Synthesized from *N*-Diazeniumdiolate-Modified Silane Precursors

Wesley L. Storm and **Mark H. Schoenfisch***
University of North Carolina at Chapel Hill, CB 3290, Chapel Hill, NC 27599

Abstract

Nitric oxide (NO)-releasing xerogel materials were synthesized using *N*-diazeniumdiolate-modified silane monomers that were subsequently co-condensed with an alkoxysilane. The NO-release characteristics were tuned by varying the aminosilane structure and concentration. The resulting materials exhibited maximum NO release totals and durations ranging from 0.45–3.2 μmol cm^{-2} and 20–90 h, respectively. The stability of the xerogel networks was optimized by varying the alkoxysilane backbone identity, water to silane ratio, base catalyst concentration, reaction time, and drying conditions. The response of glucose biosensors prepared using the NO-releasing xerogel (15 mol% *N*-diazeniumdiolate-modified *N*-2-(aminoethyl)-aminopropyltrimethoxysilane) as an outer sensor membrane was linear (R^2 = .979) up to 24 mM glucose. The sensitivity (3.4 nA mM^{-1}) of the device to glucose was maintained for 7 d in phosphate buffered saline. The facile sol-gel synthetic route, along with the NO release and glucose biosensor characteristics, demonstrates the versatility of this method for biosensor membrane applications.

Keywords

sol-gel; nitric oxide; enzymatic glucose sensor; *N*-diazeniumdiolate

Introduction

For more than half of a century, researchers have developed materials capable of controllably releasing bioactive agents in vivo.[1] While timed pharmacological release of a drug or gene were initial goals,[2] much recent work has focused on the release of therapeutics from surfaces/coatings to enhance the function and biocompatibility of a medical implant or device.[3] For example, surfaces that release antibiotics and antimicrobial agents have been studied extensively as a strategy for reducing hospital-acquired infections associated with medical devices such as stents, catheters, and orthopedic implants.[4] By foregoing traditional means of administration (e.g., oral and intravenous) and relegating the drug or agent to the membrane surface, therapeutic concentrations are maintained in the immediate vicinity of the implant while toxicity common to systemic delivery at greater doses is avoided. Nitric oxide (NO) has garnered recent attention as an active release agent due to its broad activity, short half-life, and established presence in human physiology.[4–6]

*Corresponding Author: schoenfisch@unc.edu.

ASSOCIATED CONTENT

Supporting Information. Nitric oxide storage from xerogels stored in atmospheric and vacuum conditions, silicon leaching for all pre-diazeniumdiolated compositions, elemental (CHN) analysis of xerogels, real-time NO release curves of *N*-diazeniumdiolated silanes before and after long-term storage, NO storage totals of the AEAP/NO-PTMOS sols as a function of reaction time, and cytotoxicty of leaching solutions. This material is available free of charge via the Internet at http://pubs.acs.org.

Nitric oxide is a reactive radical that modulates a seemingly interminable number of physiological processes.[7, 8] Surface-generated NO has been shown to reduce bacterial adhesion and viability, platelet adhesion, and several deleterious consequences of the foreign body response (e.g., inflammation, avascularization and collagen capsule formation).[5, 6, 9–12] As NO is a gas at ambient pressures and temperatures, its controlled release from a device or coating is best achieved chemically using donor species that decompose into NO. To this end, researchers have designed macromolecular scaffolds modified with *N*-diazeniumdiolate or *S*-nitrosothiol functional groups capable of generating NO at controlled rates (Scheme 1).[13–21]

Surfaces that slowly release NO are of particular importance for developing more biocompatible medical device coatings due to their ability to reduce biofouling and mitigate the foreign body response. The sol-gel synthesis of xerogel materials represents one method for facilitating NO release. Xerogels are attractive as biomaterials due to inherently mild synthetic conditions (eg., aqueous solvents, low temperature), a high degree of material tailorability, and the capacity for enzyme immobilization with retained enzyme activity.[22, 23] Xerogels may be prepared using any number of precursor silanes, including those necessary for storing NO (e.g., amine- and thiol-bearing silanes offer sites for *N*-diazeniumdiolate or *S*-nitrosothiol formation, respectively).[18, 21, 24] Careful selection of organically modified precursors provides a route to control surface area, pore structure, and hydrophobicity.[25] These attributes allow for the release of NO (and other therapeutic agents)[26,27,28] from the xerogel network while simultaneously allowing diffusion of external species into the xerogel. Coupling the beneficial attributes of NO release with glucose sensor membranes has thus been proposed as a means for developing more functional sensors.[29–31].

Previously, NO-releasing xerogels were prepared by forming an amine-functionalized matrix that was subsequently exposed to high pressures of NO (5 bar) to facilitate *N*-diazeniumdiolate formation.[5,10,13,22] While these films liberated NO under physiological conditions (37 °C, pH 7.4) at fluxes sufficient to reduce bacterial adhesion,[12] lower the incidence of implant infections,[5, 32] and mitigate the FBR,[11] practical issues with their synthesis limited their potential utility. First, the conversion of amines to *N*-diazeniumdiolates after film synthesis required that the underlying substrate be exposed to high pressures of NO, an impractical step for many materials and medical devices. Secondly, the *N*-diazeniumdiolate conversion efficiencies from the secondary amines to NO donors for stable compositions were only 5–25%.[21] Finally, glucose oxidase-based sensors formed using these materials were characterized as having both low glucose sensitivities and limited hydrogen peroxide permeability as a direct result of the *N*-diazeniumdiolate formation process.[31, 33]

We hypothesize that the formation of *N*-diazeniumdiolates on aminosilane precursors prior to film formation may improve glucose sensor attributes while increasing NO loading (Scheme 2). The use of different N-diazeniumdiolate precursors may also enable improved tuning of both NO release totals and durations from these materials. In contrast to post-diazeniumdiolated materials that are generally impermeable to small polar analytes such as hydrogen peroxide, we expect that pre-diazeniumdiolated xerogels not requiring exposure to high pressures of NO will function more effectively as glucose sensor membranes.

Experimental Section

Materials

N-2-(aminoethyl)-aminopropyltrimethoxysilane (AEAP), *N*-ethylaminoisobutyltrimethoxysilane (EAiB), *N*-methylaminopropyltrimethoxysilane (MAP), *N*-6-(aminohexyl)aminopropyltrimethoxysilane (AHAP), n-propyltrimethoxysilane

(PTMOS), and isobutyltrimethoxysilane (BTMOS) were purchased from Gelest (Tullytown, PA). Methyltrimethoxysilane (MTMOS), glucose oxidase, and D-glucose were purchased from Sigma Aldrich (St. Louis, MO). Nitric oxide gas was purchased from Praxair (Bethlehem, PA). Nitric oxide calibration (26.85 ppm, balance N_2) and argon gasses were purchased from Airgas National Welders (Durham, NC). Sodium methoxide (5.4 M in methanol) was purchased from Acros Organics (Fairlawn, NJ). Milli-Q water with a resistivity of <18.2 mΩ cm and a total organic content of <6 ppb was prepared by purifying distilled water using a Millipore Milli-Q UV Gradient A-10 system (Bedford, MA). Fibroblast L929 cells were acquired from the UNC tissue culture facility (Chapel Hill, NC). Dulbecco's modified essential media (DMEM), (3-(4,5-dimethylthiazol-2-yl)-5-(3-carboxymethoxyphenyl)-2-(4-sulfophenyl)-2H-tetrazolium) (MTS) and phenazine methosulfate (PMS) were acquired from Becton, Dickinson and Company (Sparks, MD). All other reagents were analytical grade and used as received.

Synthesis of *N*-diazeniumdiolate-modified Silanes and Xerogels

Preparation of N-Diazeniumdiolate-modified Aminosilanes—Silanes functionalized with *N*-diazeniumdiolates were prepared by dissolving 250 μL of the aminosilane (i.e., AEAP, EAiB, MAP) into 1750 μL of methanolic sodium methoxide (1 molar equivalent of sodium methoxide per secondary amine). The vials were placed in a 250 mL stainless steel Parr bomb, flushed with 100 psi argon for 6 cycles (three rapid, three for 10 min each), and then held at 10 bar NO for 3 d to yield the *N*-diazeniumdiolate silane form, or AEAP/NO, EAiB/NO and MAP/NO. After 3d, the vessel was purged with 100 psi argon for an additional 6 cycles (three rapid, three 10 min) prior to sample removal. Both prior to and following NO addition, great care was taken to purge the vessel slowly (~50 psi min^{-1}) to avoid solvent evaporation. Indeed, no solvent loss was observed during the *N*-diazeniumdiolate-modification process. The solutions were transferred as-is into sealed vials, placed in vacuum-evacuated foil bags ("vacuum sealed") using a commercial MiniPack-Torre MV31 vacuum sealer (Orange, CA) and stored at −20 °C until further use.

Substrate Preparation—Commercially pure, grade 3 titanium substrates (10 mm × 10 mm × 1 mm) were etched in 50% v/v sulfuric acid at 60 °C for 1 h with intermittent agitation. The substrates were then rinsed copiously with deionized water and their surfaces activated by exposing them to a solution of piranha (3 parts conc. sulfuric acid to 1 part 30% v/v hydrogen peroxide) for 10 min. Due to the highly reactive nature of this solution, care was taken to ensure that secondary containment and full personal protective equipment were used. Following additional rinsing, the substrates were ultrasonicated for 10 min in milli-Q water and stored in clean milli-Q until use.

Xerogel Synthesis—Xerogel films containing covalently bound *N*-diazeniumdiolate precursors were synthesized via a two-step, one-pot reaction by combining either AEAP/NO, MAP/NO, or EAiB/NO with pre-hydrolyzed PTMOS. First, PTMOS (117, 111, or 105 μL for 5, 10, 15%, respectively) was prehydrolyzed by adding 100 μL ethanol and 0.1 M hydrochloric acid (10 μL) and mixing for 1 h. Following pre-hydrolysis of the backbone silane, water, ethanol, base catalyst (at an excess to the initial amount of acid added so that the solution was basic) and *N*-diazeniumdiolate-modified silanes were added as follows for each system: *15 mol% MAP/NO-PTMOS*: 196 μL ethanol, 79.6 μL water, 36 μL 0.5M KOH, and 164.8 μL MAP/NO; *15 mol% EAiB/NO-PTMOS*: 166 μL ethanol, 43.6 μL water, 72 μL 0.5 M KOH, 194.8 μL EAiB/NO; *15 mol% AEAP/NO-PTMOS:* 174 μL ethanol, 23 μL water, 36 μL 0.5 M KOH, 184.8 μL AEAP/NO. For 5 and 10 mol% xerogels, one- or two-thirds volumes of the silane/NO solutions were added instead of the amounts listed above, with total volumes kept constant via the addition of pure ethanol. Following reaction,

20 μL aliquots of the resulting sol was cast onto titanium substrates, pre-dried at 60 °C for 10 min, and then further cured under vacuum at 60 °C for 3 d.

Characterization of *N*-diazeniumdiolate-modified Silanes and Xerogels

Nitric Oxide Release—Release of NO from *N*-diazeniumdiolate-modified precursor silanes and xerogels was measured using a Sievers 280 Nitric Oxide Analyzer (NOA; Boulder, CO). The NOA instrument was first calibrated using an NO zero tube (0 ppm NO) and an NO calibration tank (26.85 ppm, balance N_2). Approximately 30 mL of phosphate buffered saline (PBS; 10 mM, pH 7.4) was placed in a flask fitted with a porous frit and deoxygenated with nitrogen. During NO analysis, the instrument's flow uptake of 200 mL min^{-1} was matched by supplying nitrogen through the submerged frit at a flow rate of 80 mL min^{-1} with the remaining 120 mL min^{-1} supplied to the headspace of the vessel through a glass side arm, sweeping any liberated NO into the instrument's reaction cell. To calculate the conversion efficiency of the *N*-diazeniumdiolate NO donors, the following equation was used:

$$\%\text{conversion}=\frac{\text{moles total NO released}/2}{\text{moles total sliane}}\times 100\%$$

Spectroscopic and Mass Characterization of Precursors—Conversion of amines to *N*-diazeniumdiolate NO donors was confirmed using a Thermo Scientific Evolution Array UV-visible spectrophotometer. After reaction with NO, the aminosilane solutions were diluted to 50 μM total silane (i.e., by using the concentration of the parent aminosilane before charging) in 1.0 M sodium hydroxide. To calculate the molar absorptivity coefficient (e), the total *N*-diazeniumdiolate content was assumed to be equal to half of the total NO release (as determined via chemiluminescence).

ESI/MS was employed in positive ion mode to characterize the *N*-diazeniumdiolate-modified aminosilanes. Sodiated product ions for MAP/NO, EAiB/NO and AEAP/NO were observed at m/z 298.03 (theor. 298.08), 326.11 (theor. 326.11) and 327.10 (theor. 327.11), respectively.

Xerogel Characterization—To assess the stability of the NO-releasing xerogels, substrates were submerged in 5 mL PBS and incubated at 37 °C. Films were transferred to new soak solutions after 4 and 7 d and ultimately removed after 14 d. To quantify material stability, the Si concentrations within the soak solutions were determined using inductively coupled plasma optical emission spectrometry (ICP-OES). A standard calibration curve was constructed using 0, 500, 1000, 5000, and 10000 ppb Si (via sodium silicate) in PBS. Each mole of silicon in solution was assumed to correlate directly with silanes that disassociated from the scaffold through rehydrolysis of siloxane bonds or unreacted silanes that leached out of the matrix. Total % leaching was determined by integrating the total Si leaching concentration over the 14 d period and dividing by the number of moles of Si in each film. To determine surfaces areas, nitrogen adsorption isotherms were acquired using a Micromeretics TriStar II 3020 (Norcross, GA) and analyzed via the Brunauer-Emmet-Teller (BET) method.[34] Elemental analysis was carried out using a PerkinElmer CHN/S O elemental analyzer Series 2400 (Waltham, MA). For both elemental and BET measurements, samples were prepared by casting an equivalent volume of sol per unit area substrate onto pre-cleaned (10 min sonication in water, ethanol, and acetone) glass slides, drying accordingly, and mechanically removing the resulting films from the substrate via scraping.

Cytotoxicity—Leachate solutions (i.e., solutions that the xerogels were submerged in) from pre-diazeniumdiolated xerogels were evaluated for toxicity against L929 fibroblast cells. Leachate solutions were prepared by incubating the films for 1 week in 10 mL PBS at 37 °C. Cells were grown to confluence at 37 °C in a 5% CO_2/95% O_2 humidified environment in DMEM supplemented with 10% (v/v) fetal bovine serum (FBS) and 1 wt% penicillin/streptomycin.. Following surface desorption of the cells by trypsinization, the suspension was diluted with additional DMEM, centrifuged for 10 min (1200 rpm, 4 °C), and resuspended in an equivalent volume of media. Cells were seeded in a 96-well plate, supplying additional media and an equal volume of leachate solutions so that the total cell concentration was 3×10^5 cells mL^{-1}. Following two days of incubation at 37 °C, cell viability was determined by removing excess media and replacing with MTS/PMS reagents in DMEM. After an additional 1 h of incubation at 37 °C, the absorbance of the MTS product was measured spectrophotometrically at 490 nm using a Thermo Scientific Multiskan EX plate reader. After accounting for the absorbance from blank wells (i.e., those containing no MTS), the results were normalized to PBS controls.

Glucose Sensor Membranes

Fabrication of NO-releasing Glucose Sensors—Xerogel-coated enzymatic glucose sensors were prepared on insulated platinum disc macroelectrodes (total radius of 0.30 cm). Sol-gel immobilized glucose oxidase (GOx) was first deposited on the bare polished electrodes as described previously. , After allowing the sensing layer to dry, 6.43 μL (20 μL cm^{-2}) 15 mol% AEAP/NO-PTMOS sols were cast over the sensing layer, dried at 40 °C for 10 min and dried in vacuo at 40 °C for 3 d. Following curing, the sensors were stored at −20 °C under N2 until further use.

Sensor Performance—The analytical performance of both post-diazeniumdiolated and pre-diazeniumdiolated AEAP/NO glucose membranes was assessed using a CH Instruments 1030A potentiostat configured with a 3-electrode platform; the glucose sensor, an Ag/AgCl electrode and a platinum wire served as the working, reference, and counter electrodes, respectively. Electrodes were submerged in 50 mL of 10 mM PBS at room temperature and pre-hydrated for one hour at a potential of +0.6 V vs. Ag/AgCl. The permeability ($P_{H_2O_2}$) of each xerogel-modified electrode was determined in 10 μM H2O2 solution from the oxidation current at both bare ($\Delta i_{(bare)}$) and AEAP/NO-PTMOS-coated ($\Delta i_{(Coated)}$) electrodes using the following equation:

$$P_{H_2O_2} = \frac{\Delta i_{(\text{coated})}}{\Delta i_{(\text{bare})}} \times 100\%$$

The glucose sensing properties of the membranes were determined by adding successive aliquots of 1.0 M D-Glucose in 3 μM increments until reaching a final concentration of 30 μM.

Results and Discussion

Silane Modification with *N*-Diazeniumdiolates

Prior to xerogel formation, it was first necessary to prepare and characterize the *N*-diazeniumdiolate-functionalized aminosilane precursors. We hypothesized that significant NO loading would occur on the aminosilane precursors when exposed to NO in the presence of exogenous base. Solvent type as well as aminosilane and sodium methoxide concentrations were varied to maximize amine to *N*-diazeniumdiolate NO donor conversion efficiencies while minimizing the formation of byproducts. Initially, ethanol and methanol

were tested; however, ethanol formed an NO-releasing byproduct under the conditions used herein.[35] Thus, only methanol was employed. Methanol proved superior as the solvent as it dissolved both the sodium methoxide base and each aminosilane (structures illustrated in Figure 1) successfully. In the absence of sodium methoxide, intramolecular amines in the AEAP precursor are able to serve as bases. Nevertheless, negligible diazeniumdiolate formation was observed as calculated from NO-release data (~5.3% conversion efficiency), indicating the need for a stronger base to optimize NO loading in methanol. Although reports have indicated the formation of sodium formate from methoxide and NO,[36] this byproduct does not decompose to release NO and is thus considered benign for our purposes. The alternative base suggested by DeRosa and coworkers (i.e., sodium trimethylsilanolate) is not compatible with silanes as it reacts to form polysiloxanes.[37] As such, all further *N*-diazeniumdiolate-modified silane preparation was carried out using 12.5% (v/v) aminosilane in methanol with 1.0 molar equivalent sodium methoxide per secondary amine.

Nitric oxide release totals and kinetics from *N*-diazeniumdiolate-modified silanes were characterized using chemiluminescence.[38] As provided in Table 1, *N*-diazeniumdiolate formation and subsequent NO release (theoretical release of two mol NO per mol of *N*-diazeniumdiolate NO donor) varied significantly with the structure of the precursor aminosilane. The conversion of secondary amines to *N*-diazeniumdiolate NO donors was greatest for the monoamines (MAP and EAiB at ~70%) and least for the diamine AEAP (~50%). The lower conversion for AEAP is attributed to stabilization of 2° amines by neighboring 1° amines. While changes in chemical structure may impact the NO addition efficiency, they also control the resulting NO-release kinetics. For example, the NO release from EAiB/NO had a slightly longer $t_{1/2}$ than MAP/NO (7.9 and 2.0 min, respectively), due to increased organic character protecting the *N*-diazeniumdiolate from proton-initiated decomposition. The diamine-based aminosilane in this study, AEAP/NO, exhibited an NO release half-life of more than an order of magnitude longer (120 min) than either of the monoamine silanes as a result of hydrogen-bonding stabilization from the 1° amine.[39]

The presence of a strong UV absorption band at a wavelength of ~250 nm confirmed successful *N*-diazeniumdiolate NO donor formation (Figure 2). Molar absorptivity coefficients (ε, Table 1) were calculated by using the absorbance at λ_{max} along with *N*-diazeniumdiolate concentrations inferred through chemiluminescent NO release totals. For all silanes, the molar absorptivity coefficients proved to be within the range of previously observed values ($7 – 20\ mM^{-1}\ cm^{-1}$).[40, 41]

The long-term stability of the precursor solutions was evaluated by measuring their NO release after approximately 6 months of storage in a vacuum sealed container at −20 °C. The change in the resulting NO-release profiles was minimal for each system (Figure S1 in Supporting Information). As a result, long-term storage did not hamper NO-release capacity from the xerogels formed using these precursors.

Xerogel Synthesis

Successful formation of stable *N*-diazeniumdiolate-modified xerogels required study of several reaction parameters in the initial sol including backbone silane identity, aminosilane concentration, acid and base catalyst concentration, water:silane ratio, and reaction time. Both the stability of the resulting xerogel framework and the *N*-diazeniumdiolate groups contained within were evaluated upon all synthetic variations. Titanium was chosen as the substrate for the materials due to its common use in biomedical implants and ability to stably adhere the xerogel films.[42]

Although sol-gel synthesis of xerogels often employs only an acid catalyst, a base catalyst had to be incorporated during this synthesis to avoid proton-initiated decomposition of the *N*-diazeniumdiolate NO donors. Initially, a one-step hydrolysis and co-condensation of the backbone and *N*-diazeniumdiolate-modified silanes under basic conditions was attempted. While films synthesized in this manner appeared well-cured on the benchtop, xerogels made from this procedure were unstable when submerged in PBS (~20% total Si leached into solution). This instability is attributed to inadequate connectivity between the backbone silane (PTMOS) and the aminosilane. Indeed, previous reports have indicated the importance of well-matched reaction kinetics when co-condensing alkoxysilanes via the sol-gel method.[43] To remedy this instability, a two-step reaction was adapted to fabricate xerogels with *N*-diazeniumdiolated silane concentrations of up to 15 mol%. Of note, larger concentrations yielded physically unstable xerogels regardless of the synthetic strategy employed. As aminosilanes exhibit faster gelation times than n-alkylated silanes,[44] the PTMOS backbone was first pre-hydrolyzed in 4.9 mM HCl prior to the addition of the *N*-diazeniumdiolated aminosilane. Further increasing acid concentrations to 24.5 mM and 49.0 mM HCl destabilized the xerogel (as determined via leaching), suggesting that hydrolysis and condensation rates are well-matched at the optimal acid concentration of 4.9 mM. Experiments conducted with other backbone silanes also illustrated the need for similar hydrolysis and condensation rates. For example, the xerogels displayed a significant amount of cracking, even at relatively low water:silane ratios (3.2) and reaction times (1 h), when 15 mol% AEAP/NO, MAP/NO, and EAiB/NO films were synthesized using an MTMOS backbone. Conversely, films synthesized using bulkier BTMOS did not adequately cure and remained highly viscous and tacky even after catalyst-assisted reaction and drying. When using PTMOS as the backbone, stable, non-tacky films were synthesized by adjusting water:silane ratios. For AEAP/NO-PTMOS, 3.2 H_2O:Si was ideal, while 10:1 ratios of H_2O:Si were necessary to form stable MAP/NO-PTMOS and EAiB/NO-PTMOS xerogels. Reactions involving EAiB/NO were particularly torpid, requiring an additional increase in base catalyst concentration for adequate cocondensation. The bulky, hydrophobic nature of EAiB/NO-PTMOS, and to a lesser extent MAP/NO-PTMOS, xerogels was further evidenced by xerogel opacity that developed after extended soaking in PBS. As these films were translucent in dry, ambient conditions, this is strong evidence of microsyneresis—a phenomenon that occurs in organic gels when a polymer exhibits greater affinity for itself than its surrounding solvent (i.e., a hydrophobic polymer surrounded by water).[45]

Xerogel NO Release

We hypothesized that xerogels synthesized from *N*-diazeniumdiolate-modified silanes would provide enhanced NO loading per amine relative to post-diazeniumdiolated xerogels. Post-diazeniumdiolated xerogels rely on deprotonation by neighboring amines within the scaffold to facilitate xerogel formation. Thus, NO release is limited by base (i.e., internal amine) availability. Addition of exogenous bases is not feasible, as silica constructs are often unstable in high pH conditions.[25] Since the xerogels in this work were synthesized from silanes converted to *N*-diazeniumdiolates prior to network formation, conversion of secondary amines to *N*-diazeniumdiolates was enhanced without compromising network stability. To confirm this hypothesis, the NO release from pre-diazeniumdiolated xerogels was measured in physiologically relevant conditions (PBS at 37 °C and pH 7.4) using chemiluminescence (NOA) and compared to that of post-diazeniumdiolated xerogels.

As expected, 15 mol% pre-diazeniumdiolated xerogels released orders of magnitude more NO than post-diazeniumdiolated xerogels at equivalent aminosilane mol percentages (Table 3). This increase was greatest for MAP/NO-PTMOS and EAiB/NO-PTMOS xerogels due to their low NO donor conversion efficiencies when post-diazeniumdiolated—a finding consistent with the hypothesis that amines within the xerogels are responsible for

deprotonation necessary for *N*-diazeniumdiolate formation. When diamine-containing xerogels are post-diazeniumdiolated, the overall amine content is larger and the close proximity of intramolecular amines makes deprotonation more likely. In turn, post-diazeniumdiolated AEAP/NO-PTMOS xerogels release more NO than post-diazeniumdiolated MAP/NO-PTMOS and EAiB/NO-PTMOS. Nonetheless, each pre-diazeniumdiolated xerogel system studied released greater levels of NO than post-diazeniumdiolated systems (at equivalent mol%).

With respect to NO totals, the pre-diazeniumdiolated AEAP/NO-PTMOS, MAP/NO-PTMOS, and EAiB/NO-PTMOS xerogels released 2.6, 2.4, and 3.2 μmol NO cm^{-2}, respectively. When synthesized with 15 mol% *N*-diazeniumdiolated silane precursors, the NO storage capacity (i.e., the percentage of secondary amines that are *N*-diazeniumdiolate-modified) of these xerogels was 52.8% for EAiB/NO-PTMOS and approximately ~40% for both AEAP/NO-PTMOS and MAP/NO-PTMOS xerogels. These losses are a result of both incomplete conversion of the precursors and *N*-diazeniumdiolate degradation during synthesis (Table 1 and Table 3). Of note, AEAP/NO-PTMOS and MAP/NO-PTMOS released equivalent levels of NO (2.40 and 2.60 μmol cm^{-2}, respectively) despite the much greater 74% conversion efficiency of secondary amines to *N*-diazeniumdiolates in the MAP/NO precursor (compared to 49% for AEAP/NO). This disparity is best explained by the fast release kinetics of the MAP/NO small molecule. While NO donor degradation during reaction of the sol was negligible (Figure S2 in Supporting Information), a significant loss of NO occured during the initial 10 min of drying. Such NO loss ceases once the materials/coatings are placed under vacuum. Thus, NO loss during synthesis will be most drastic for those systems with rapid *N*-diazeniumdiolate decomposition kinetics. As such, NO retention (i.e., the percentage of *N*-diazeniumdiolates remaining after xerogel synthesis) is greatest for AEAP/NO-PTMOS and EAiB/NO-PTMOS xerogels at 80.7 and 74.9%, respectively, and least (56.8%) for MAP/NO-PTMOS xerogels (Table 3).

Elemental analysis of the xerogel films (see Supporting Information) confirmed that the mass percentage of nitrogen (%N) in the xerogels increased with increasing mol% of *N*-diazeniumdiolated precursors. As expected from its diamine structure, 15 mol% AEAP/NO-PTMOS xerogels were found to have the largest %N. In using the %N in each xerogel to calculate a theoretical NO release, it was found that CHN overestimated NO totals by 16–35%. We attribute this difference to residual nitrite in the matrix that is present from NO loss during synthesis. Supporting this hypothesis, the magnitude by which this overestimation occurs for each system trends remarkably well with the amount of NO lost during synthesis for the respective systems (MAP/NO-PTMOS > EAiB/NO-PTMOS > AEAP/NO-PTMOS).

The NO release from the *N*-diazeniumdiolate-modified xerogels synthesized in this work was tunable by varying the aminosilane identity. As shown in Table 2, MAP/NO-PTMOS xerogels have the shortest NO release half-lives (1.9 h) and durations (35.7 h), consistent with the rapid decomposition of the MAP/NO precursor. While MAP/NO has an NO-release half-life nearly 60 times lower than AEAP/NO (2.0 and 130 min, respectively), this difference is much less pronounced from the xerogels themselves. The NO-release half-life of the AEAP/NO- PTMOS xerogels was only twice as long as MAP/NO-PTMOS xerogels, demonstrating that the hydrophobicity of the xerogel matrix has a significant influence on the NO release rates versus any intramolecular *N*-diazeniumdiolate stabilization by 1° amines. The non-polar EAiB/NO precursor clearly increased matrix hydrophobicity (evidenced by the microsyneresis phenomenon described above), slowing NO release kinetics. Others have reported the accumulation of hydroxide ions within hydrophobic NO-donor matrices as the *N*-diazeniumdiolates decompose.[6] This phenomenon would further contribute to prolonged NO release due to enhanced *N*-diazeniumdiolate donor stability at

elevated pH. The longer NO-release duration (90.8 h) for 15 mol% EAiB/NO-PTMOS xerogels would thus be expected relative to the other systems.

The largest maximum NO flux obtainable using these materials (590 pmol cm^{-2} s^{-1}) exceeds the flux required for a ~90% reduction in bacterial adhesion in vitro (25–30 pmol cm^{-2} s^{-1} for *E. coli, S. aureus, and P. aeruginosa*).[4, 46] The maximum NO fluxes from each film (Table 2 and Figure S3 in Supporting Information) potentially raise concerns, as large NO concentrations may promote undesirable inflammation.[47] However, previous studies have assesed the FBR as a function of NO-release kinetics, and demonstrated no ill effect on localized inflammation for materials with far greater maximum NO fluxes (~1440 pmol cm^{-2} s^{-1} vs. 700 pmol cm^{-2} s^{-1} for the xerogels herein).[10] Of note, the 15 mol% xerogel systems presented above have NO-release properties and kinetics comparable to NO-releasing polyurethane membranes reported to reduce in vivo inflammation and collagen capsule thickness (total NO = 3.0 μmol cm^{-2} and NO flux at 48 h = 1.13 pmol cm^{-2} s^{-1}).[10]

As detailed earlier, xerogels synthesized using *N*-diazeniumdiolate-modified silanes exhibited physical instability (i.e., fragmentation in aqueous solution) when formed with concentrations exceeding of 15 mol%. In contrast, stable post-diazeniumdiolated xerogels have been reported up to concentrations of approximately 30 mol%.[21] As such, the NO release of pre-diazeniumdiolated xerogels at their highest mole percentage were compared to materials containing even greater mole percentages of post-diazeniumdiolated xerogels. Using a similar two-step reaction, post-diazeniumdiolated xerogels prepared using AHAP (40 vol%, 31 mol%) and BTMOS demonstrated efficacy in combatting bacterial and fungal adhesion in vitro, preventing infection, and alleviating the foreign body response in vivo.[5, 11, 12, 48] This system released a total of 3.3 ± 0.6 μmol NO cm^{-2}, nearly equivalent to the 15 mol% EAiB/NO xerogels synthesized herein. The similar NO release totals between these two systems illustrates the larger conversion efficiency of pre-diazeniumdiolated xerogel systems, despite the difference in total aminosilane incorporation.

Xerogel Stability

To assess the physical stability of the *N*-diazeniumdiolate-modified xerogels, films were immersed in PBS (pH 7.4, 37 °C) for 4, 7, and 14 d. Subsequent analysis of the soak solutions was carried out using ICP-OES. The amount of silicon in the solutions was assumed to correlate to silane leaching from the silica network, and would represent poor physical integrity of the xerogels upon solution immersion. As shown in Figure 3 and Table S2 (Supporting Information), the xerogels leached <5 mol% of their total silicon content, indicating excellent stability under these solution conditions. Marxer and coworkers characterized leaching in a similar manner from post-diazeniumdiolated xerogels.[21] While one composition (40% AEMP/BTMOS) only exhibited <0.5 mol% Si loss after two weeks, 40% AHAP/BTMOS films lost 8.3 mol% Si content after two weeks in 37 °C PBS.[21] To evaluate the potential cytotoxicity of these systems, we tested leaching solutions from the largest mol% xerogel of each aminosilane (corresponding to the films with the greatest degree of instability) against L929 murine fibroblast cells. After 24 hours of exposure to an equal volume of leachate solution and media, no significant toxicity was observed relative to PBS controls (see Figure S4 in Supporting Information) indicating negligible leaching.

In addition to the physical stability of the silica network, the chemical stability of the *N*-diazeniumdiolate functionalities within the xerogel was also considered. Release of NO from pre-diazeniumdiolated 15 mol% AEAP/NO-PTMOS xerogels was measured immediately following xerogel synthesis and again following 10 d of vacuum-sealed storage at −20 °C, vacuum sealed storage at room temperature, and storage under ambient conditions. No significant reduction in NO storage was observed when the xerogels were vacuum sealed, regardless of temperature. Xerogels stored on the benchtop (and thus

exposed to ambient humidity) lost ~60% NO over the same period (see Table S4 in Supporting Information). While decomposition of the *N*-diazeniumdiolate NO donors in solution is strongly dependent on temperature, elevated temperatures alone were not observed to initiate NO release until a certain threshold (typically much larger temperature) is reached. For example, Batchelor and coworkers observed the decomposition of lipophilic *N*-diazeniumdiolate compounds at temperatures above 104 °C.[49] Thus, storage in a vacuum-sealed container, free from water, is sufficient for maintaining NO storage for the materials described herein.

Electrochemical Glucose Sensor Membranes

Nitric oxide has a number of properties that make it favorable for release from the surface of an implanted electrochemical sensor. For example, several problems that disrupt these devices such as excessive collagen encapsulation, avascularization, and infection are mitigated through the release of NO.[50] In prior work, we reported that glucose biosensors coated with post-diazeniumdiolated xerogels exhibited poor sensitivity to glucose.[31, 33] This result was attributed to decreased analyte permeability through the sensor membrane after NO charging. Shin and colleagues hypothesized that NO catalyzed xerogel condensation, thus reducing the overall porosity of the material and greatly limiting analyte (e.g., glucose permeability.[31] We hypothesized that these pre-diazeniumdiolated xerogels might have greater porosity than post-diazeniumdiolated xerogels due to slower hydrolysis and condensation reactions. In this respect, the coatings would prove useful as outer glucose sensor membranes.[51] Electrochemical glucose biosensors were fabricated with xerogel membranes synthesized from *N*-diazeniumdiolate-modified xerogels; specifically, 15 mol% AEAP/NO-PTMOS was used as it represented a highly stable system. A two-layer sensor membrane was cast onto a platinum disc working electrode with an Ag/AgCl reference. The bottom layer contained glucose oxidase immobilized within an MTMOS sol-gel, while either a pre-diazeniumdiolated or post-diazeniumdiolated 15 mol% AEAP/NO-PTMOS xerogel comprised the outer-most layer. This two-layer approach mirrors previous work carried out by our laboratory previously.[30, 31, 33]

The hydrogen peroxide (H_2O_2) permeability of the NO-releasing sensor membranes was determined by measuring the oxidation current for the xerogel-modified electrodes relative to bare electrodes at +0.6 V (vs. Ag/AgCl). Consistent with previous work, post-diazeniumdiolated sensor membranes exhibited responses below our limit of detection ($P_{H_2O_2} < 0.01\%$). As expected, the $P_{H_2O_2}$ for pre-diazeniumdiolated xerogels was more than an order of magnitude larger. To determine if a larger overall surface area explained the enhanced permeability, the specific surface area of pre-diazeniumdiolated xerogels was measured and compared to post-diazeniumdiolated xerogels. Indeed, the specific surface area of post-diazeniumdiolated 15 mol% AEAP/NO-PTMOS was <0.1 $m^2\ g^{-1}$ while the specific surface area of its pre-diazeniumdiolated equivalent was 2.1 $m^2\ g^{-1}$.

Next, we determined if the increased permeability led to an improved sensor response. Using the same electrode configuration, D-glucose was added to PBS to achieve final glucose concentrations from 3 to 30 mM. Of note, +0.6 V was employed as the working electrode potential to limit interference by oxidation of NO.[29, 30] Perhaps not surprising given the increased analyte permeability, sensors fitted with pre-diazeniumdiolated xerogel membranes featured larger glucose sensitivities than post-diazeniumdiolated xerogels (3.4 nA mM^{-1} and < 0.1 nA mM^{-1}, respectively). Consistent with this observation, previously reported post-diazeniumdiolated xerogels (20 mol% AEAP, balance BTMOS) constructed by Schoenfisch and coworkers suffered from a similarly low glucose sensitivity (0.14 nA mM^{-1}) that was addressed via inclusion of a hydrophilic polymer within the xerogel membrane.[33] When compared to other sensors that do not generate NO, the sensitivity observed using 15% AEAP/NO-PTMOS membranes was similar in magnitude.[52, 53]

To verify the viability of these membranes for continuous glucose monitoring, glucose measurements were repeated after soaking the electrodes in PBS for 4 and 7 d. As illustrated in Table 4, the change in glucose sensitivity was only 3.6% after one week of soaking in physiological buffer. With increasing soak time the dynamic range increased and the glucose response time decreased, likely a result of greater hydration of the enzymatic membrane over time. Nonetheless, the membranes proved functional over clinically relevant diabetic patient glucose concentrations without pre-soaking beyond the 3 h pre-hydration period. The in vitro sensitivity reported here is similar to NO-releasing sensors evaluated by Gifford and coworkers (4.88 – 6.77 nA mM^{-1}) that functioned reliably when implanted percutaneously in rats.[29] Although the response times of the sensors herein are slower (274 – 530 s compared to 75 s), the NO release durations of these sensors are nearly 2.5 times longer. These response times are not prohibitive to glucose sensor development; others have reported success (as determined via Clarke error grid analysis) using subcutaneously implanted glucose sensors with in vitro response time of ~10 min in humans.[54]

Of note, functional NO-releasing glucose sensors have been fabricated using other synthetic strategies. Silica xerogels doped with poly(vinylpyrrolidone) were shown to overcome the permeability limitations resulting from post-diazeniumdiolation.[31] While this strategy improved sensor response (sensitivity) from ~0.14 to 4.6 nA mM^{-1}, the NO storage was much less than that from the pre-diazeniumdiolated xerogels. As an alternative to silica-based xerogels, glucose sensors have also been fabricated using NO-releasing silica-modified polyurethanes.[30, 31] Polyurethanes modified with NO-releasing nanoparticles demonstrate similar NO-release totals (~2 μmol cm^{-2} s^{-1}) and glucose sensitivities (7.3–14.5 nA mM^{-1}) for sensors covering equivalent dynamic ranges.[30] While both strategies are promising, the direct synthetic route of *N*-diazeniumdiolate-modified xerogels offers a more facile approach to preparing the NO-releasing sensor membrane.

Conclusions

Sol-gel chemistry allows for the design of surfaces that release bioactive agents using facile synthetic methods with mild reaction conditions and easily obtainable precursors. Herein, xerogels fabricated from *N*-diazeniumdiolate-modified silanes were demonstrated useful for storing and releasing NO in a concentration-dependent manner, with NO-release kinetics dependent on the identity of the donor. At equivalent mole percentages, pre-diazeniumdiolated xerogels release significantly more NO (>10x) than their post-diazeniumdiolated counterparts and pre-diazeniumdiolated xerogels containing 15 mol% of the NO donor released similar amounts of NO as ~30 mol % NO donor films that are post-diazeniumdiolated. Unlike post- diazeniumdiolated films, the sensors herein function as glucose sensor membranes, operating over a clinically relevant glucose range with adequate glucose sensitivity and response for up to 1 week. To achieve larger NO-storage capacity without compromising matrix stability, future work should focus on methods for isolating the *N*-diazeniumdiolate-modified silanes before using the precursors to form xerogels. If longer NO-release durations are desired, the purification of more stable intramolecular *N*-dizeniumdiolate-modified silanes may be an important strategy. Overall, the one-pot reaction used herein provides a simple and effective strategy for fabricating NO-releasing glucose sensors. To further demonstrate the utility of these coatings for other applications, future work should make use of alternative coating methods (i.e., spraycoating and dipcoating) with a variety of substrate types and geometries.

Supplementary Material

Refer to Web version on PubMed Central for supplementary material.

Acknowledgments

This research was supported by the National Institutes of Health (NIH EB000708). WLS also wishes to acknowledge funding from Novan, Inc.

REFERENCES

1. Hoffman AS. J. Control. Release. 2008; 132:153–163. [PubMed: 18817820]
2. Rosen H, Abribat T. Nat. Rev. Drug. Discov. 2005; 4:381–385. [PubMed: 15864267]
3. Wu P, Grainger DW. Biomaterials. 2006; 27:2450–2467. [PubMed: 16337266]
4. Hetrick EM, Schoenfisch MH. Chem. Soc. Rev. 2006; 35:780–789. [PubMed: 16936926]
5. Nablo BJ, Prichard HL, Butler RD, Klitzman B, Schoenfisch MH. Biomaterials. 2005; 26:6984–6990. [PubMed: 15978663]
6. Mowery KAH, Schoenfisch M, Saavedra JE, Keefer LK, Meyerhoff ME. Biomaterials. 2000; 21:9–21. [PubMed: 10619674]
7. Nichols SP, Storm WL, Koh A, Schoenfisch MH. Adv. Drug. Deliver. Rev. 2012; 64:1177–1188.
8. Carpenter AW, Schoenfisch MH. Chem. Soc. Rev. 2012; 41:3742–3752. [PubMed: 22362384]
9. Nablo BJ, Chen TY, Schoenfisch MH. J. Am. Chem. Soc. 2001; 123:9712–9713. [PubMed: 11572708]
10. Nichols SP, Koh A, Brown NL, Rose MB, Sun B, Slomberg DL, Riccio DA, Klitzman B, Schoenfisch MH. Biomaterials. 2012; 33:6305–6312. [PubMed: 22748919]
11. Hetrick EM, Prichard HL, Klitzman B, Schoenfisch MH. Biomaterials. 2007; 28:4571–4580. [PubMed: 17681598]
12. Hetrick EM, Schoenfisch MH. Biomaterials. 2007; 28:1948–1956. [PubMed: 17240444]
13. Stasko NA, Schoenfisch MH. J. Am. Chem. Soc. 2006; 128:8265–8271. [PubMed: 16787091]
14. Shin JH, Metzger SK, Schoenfisch MH. J. Am. Chem. Soc. 2007; 129:4612–4619. [PubMed: 17375919]
15. Coneski PN, Nash JA, Schoenfisch MH. ACS Appl. Mater. Interfaces. 2012; 3:426–432. [PubMed: 21250642]
16. Lu Y, Sun B, Li C, Schoenfisch MH. Chem. Mater. 2011; 23:4227–4233. [PubMed: 22053127]
17. Riccio DA, Schoenfisch MH. Chem. Soc. Rev. 2012; 41:3731–3741. [PubMed: 22362355]
18. Riccio DA, Coneski PN, Nichols SP, Broadnax AD, Schoenfisch MH. ACS Appl. Mater. Interfaces. 2012; 4:796–804. [PubMed: 22256898]
19. Wold KA, Damodaran VB, Suazo LA, Bowen RA, Reynolds MM. ACS Appl. Mater. Interfaces. 2012; 4:3022–3030.
20. Harding JL, Reynolds MM. J. Am. Chem. Soc. 2012; 134:3330–3333. [PubMed: 22263610]
21. Marxer SM, Rothrock AR, Nablo BJ, Robbins ME, Schoenfisch MH. Chem. Mater. 2003; 15:4193–4199.
22. Dave BC, Dunn B, Valentine JS, Zink JI. Anal. Chem. 1994; 66:1120A–1127A.
23. Braun S, Rappoport S, Zusman R, Avnir D, Ottolenghi M. Mater. Lett. 1990; 10:1–5.
24. Riccio DA, Dobmeier KP, Hetrick EM, Privett BJ, Paul HS, Schoenfisch MH. Biomaterials. 2009; 30:4494–4502. [PubMed: 19501904]
25. Lev O, Tsionsky M, Rabinovich L, Glezer V, Sampath S, Pankratov I, Gun J. Anal. Chem. 1995; 67:22A–30A.
26. Stobie N, Duffy B, McCormack DE, Colreavy J, Hidalgo M, McHale P, Hinder SJ. Biomaterials. 2008; 29:963–969. [PubMed: 18061256]
27. Quintanar-Guerrero D, Ganem-Quintanar A, Nava-Arzaluz MG, Piñón-Segundo E. Expert Opin. Drug. Del. 2009; 6:485–498.
28. Iafisco M, Margiotta N. J. Inorg. Biochem. 2012; 117:237–247. [PubMed: 22824154]
29. Gifford R, Batchelor MM, Lee Y, Gokulrangan G, Meyerhoff ME, Wilson GS. J. Biomed. Mater. Res. 2005; 75A:755–766.

30. Koh A, Riccio DA, Sun B, Carpenter AW, Nichols SP, Schoenfisch MH. Biosens. Bioelectron. 2011; 28:17–24. [PubMed: 21795038]
31. Shin JH, Marxer SM, Schoenfisch MH. Anal. Chem. 2004; 76:4543–4549. [PubMed: 15283600]
32. Holt J, Hertzberg B, Weinhold P, Storm W, Schoenfisch M, Dahners L. J. Orthop. Trauma. 2011; 25:432–437. [PubMed: 21637124]
33. Schoenfisch MH, Rothrock AR, Shin JH, Polizzi MA, Brinkley MF, Dobmeier KP. Biosens. Bioelectron. 2006; 22:306–312. [PubMed: 16483759]
34. Brunauer S. J. Am. Chem. Soc. 1938; 60:309–319.
35. Traube W. Justus Liebigs Ann. Chem. 1898; 300:81–128.
36. DeRosa F, Keefer LK, Hrabie JA. J. Org. Chem. 2008; 73:1139–1142. [PubMed: 18184006]
37. Sommer LH, Pietrusza EW, Whitmore FC. J. Am. Chem. Soc. 1946; 68:2282–2284.
38. Coneski PN, Schoenfisch MH. Chem. Soc. Rev. 2012; 41:3753–3758. [PubMed: 22362308]
39. Hrabie JA, Klose JR, Wink DA, Keefer LK. J. Org. Chem. 1993; 58:1472–1476.
40. Reynolds MM, Zhou Z, Oh BK, Meyerhoff ME. Org. Lett. 2005; 7:2813–2816. [PubMed: 15987143]
41. Keefer LK, Flippen-Anderson JL, George C, Shanklin AP, Dunams TM, Christodoulou D, Saavedra JE, Sagan ES, Bohle DS. Nitric Oxide-Biol. Chem. 2001; 5:377–394.
42. Niinomi M. Mat. Sci. Eng. AStruct. 1998; 243:231–236.
43. Schubert U, Huesing N, Lorenz A. Chem. Mater. 1995; 7:2010–2027.
44. Osterholtz FD, Pohl ER. J. Adhes. Sci. Technol. 1992; 6:127–149.
45. Brinker, CJ.; Scherer, GW. Sol-gel science : the physics and chemistry of sol-gel processing. Boston: Academic Press; 1990.
46. Charville GW, Hetrick EM, Geer CB, Schoenfisch MH. Biomaterials. 2008; 29:4039–4044. [PubMed: 18657857]
47. Grisham MB, Jourd'Heuil D, Wink DA. Am. J. Physiol. Gastrointest. Liver Physiol. 1999; 276:G315–G321.
48. Privett BJ, Nutz ST, Schoenfisch MH. Biofouling. 2010; 26:973–983. [PubMed: 21082455]
49. Batchelor MM, Reoma SL, Fleser PS, Nuthakki VK, Callahan RE, Shanley CJ, Politis JK, Elmore J, Merz SI, Meyerhoff ME. J. Med. Chem. 2003; 46:5153–5161. [PubMed: 14613318]
50. Nichols SP, Koh A, Storm WL, Shin JH, Schoenfisch MH. Chem. Rev. 2013; 113:2528–2549. [PubMed: 23387395]
51. Shin JH, Schoenfisch MH. Analyst. 2006; 131:609–615. [PubMed: 16795923]
52. Dempsey E, Diamond D, Smyth MR, Urban G, Jobst G, Moser I, Verpoorte EMJ, Manz A, Michael Widmer H, Rabenstein K, Freaney R. Anal. Chim. Acta. 1997; 346:341–349.
53. Bindra DS, Zhang Y, Wilson GS, Sternberg R, Thevenot DR, Moatti D, Reach G. Anal. Chem. 1991; 63:1692–1696. [PubMed: 1789439]
54. Gilligan BC, Shults M, Rhodes RK, Jacobs PG, Brauker JH, Pintar TJ, Updike SJ. Diabetes. Technol. The. 2004; 6:378–386.

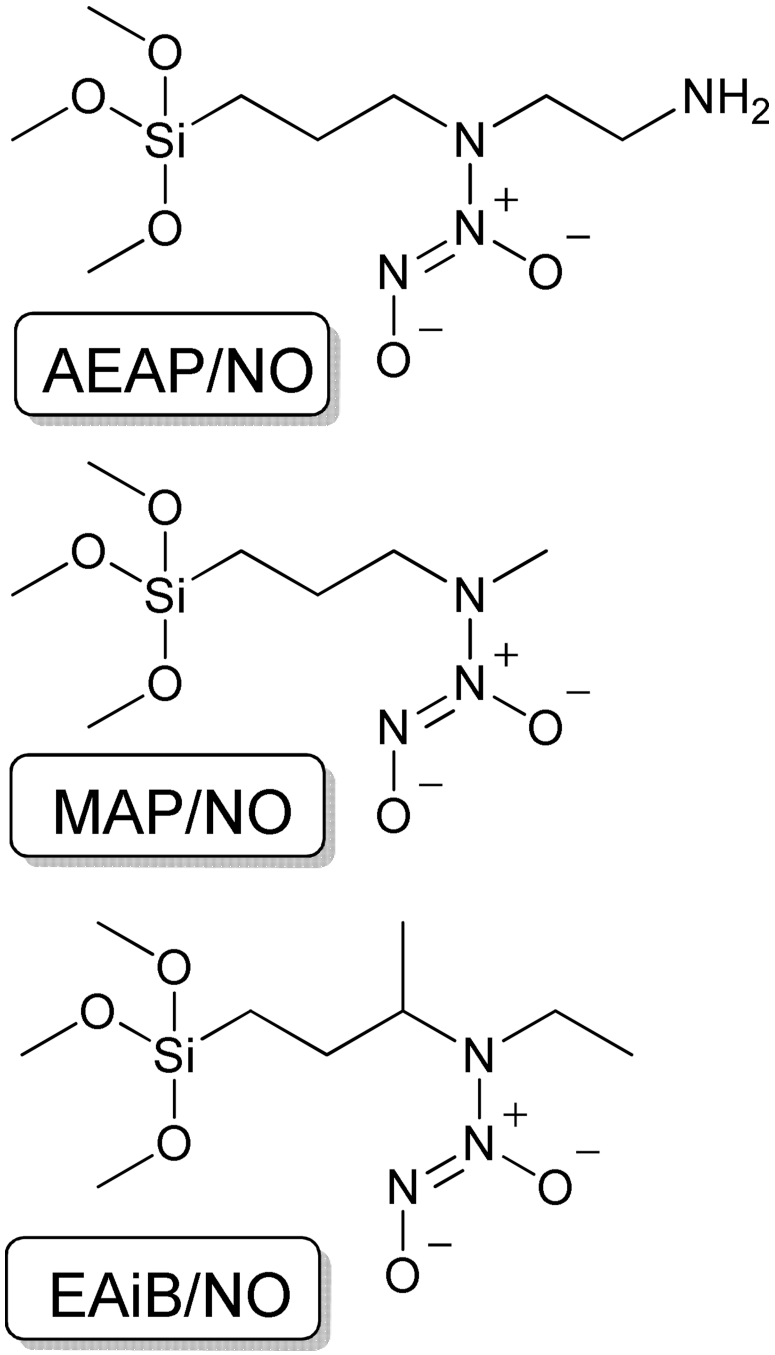

Figure 1.
Chemical structures of the *N*-diazeniumdiolate-modified aminosilanes used to fabricate NO-releasing xerogels.

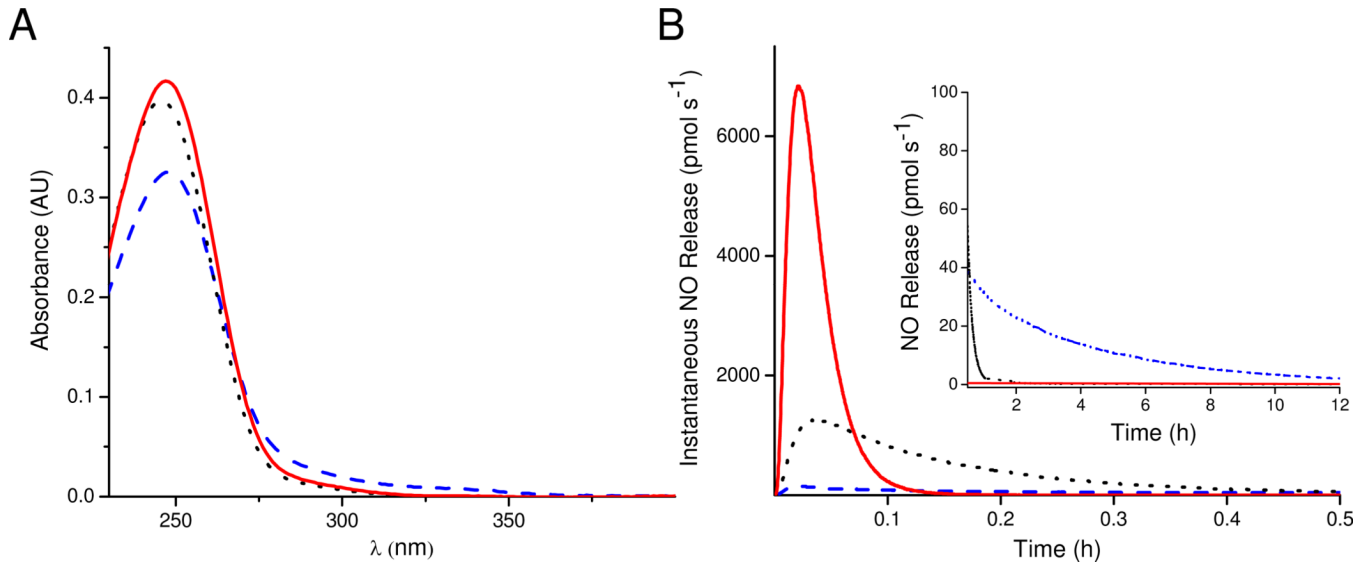

Figure 2.

A) UV-vis spectra and B) NO-release curves of AEAP/NO (blue dashed line), MAP/NO (red solid line), and EAiB/NO (black dotted line) precursors. Absorption spectra were obtained at a concentration of 50 mM in 1 M NaOH. Nitric oxide release was measured in PBS (pH 7.4, 10 mM).

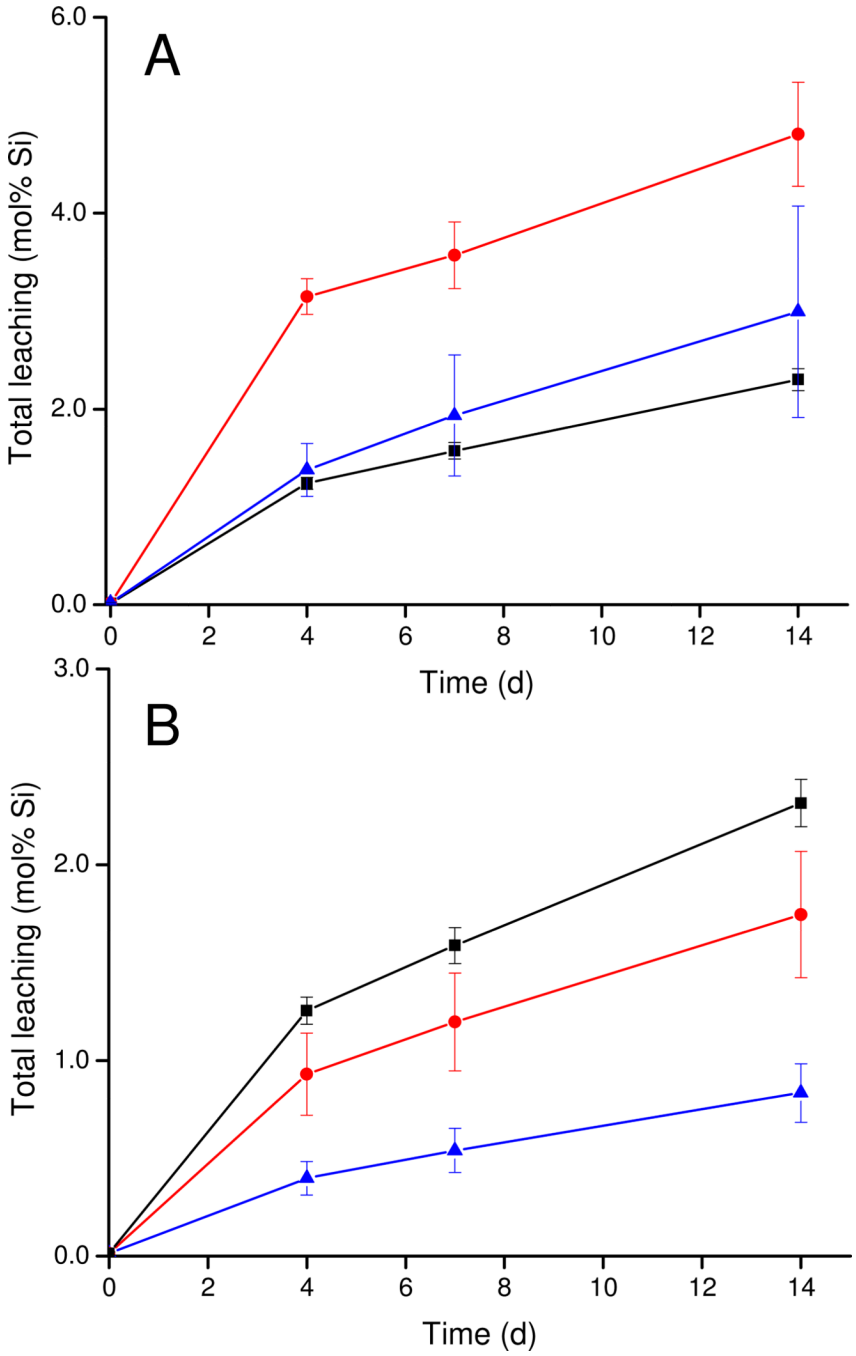

Figure 3.
Silicon leaching from pre-diazeniumdiolated xerogels as a function of NO donor A) identity and B) concentration. Silicon content was measured at 4, 7, and 14 d from A) 15 mol% AEAP/NO-PTMOS (black square), MAP/NO-PTMOS (red diamond), and EAiB/NO-PTMOS (blue triangle) and B) 5 (blue triangle), 10 (red diamond) and 15 mol% (black square) AEAP.

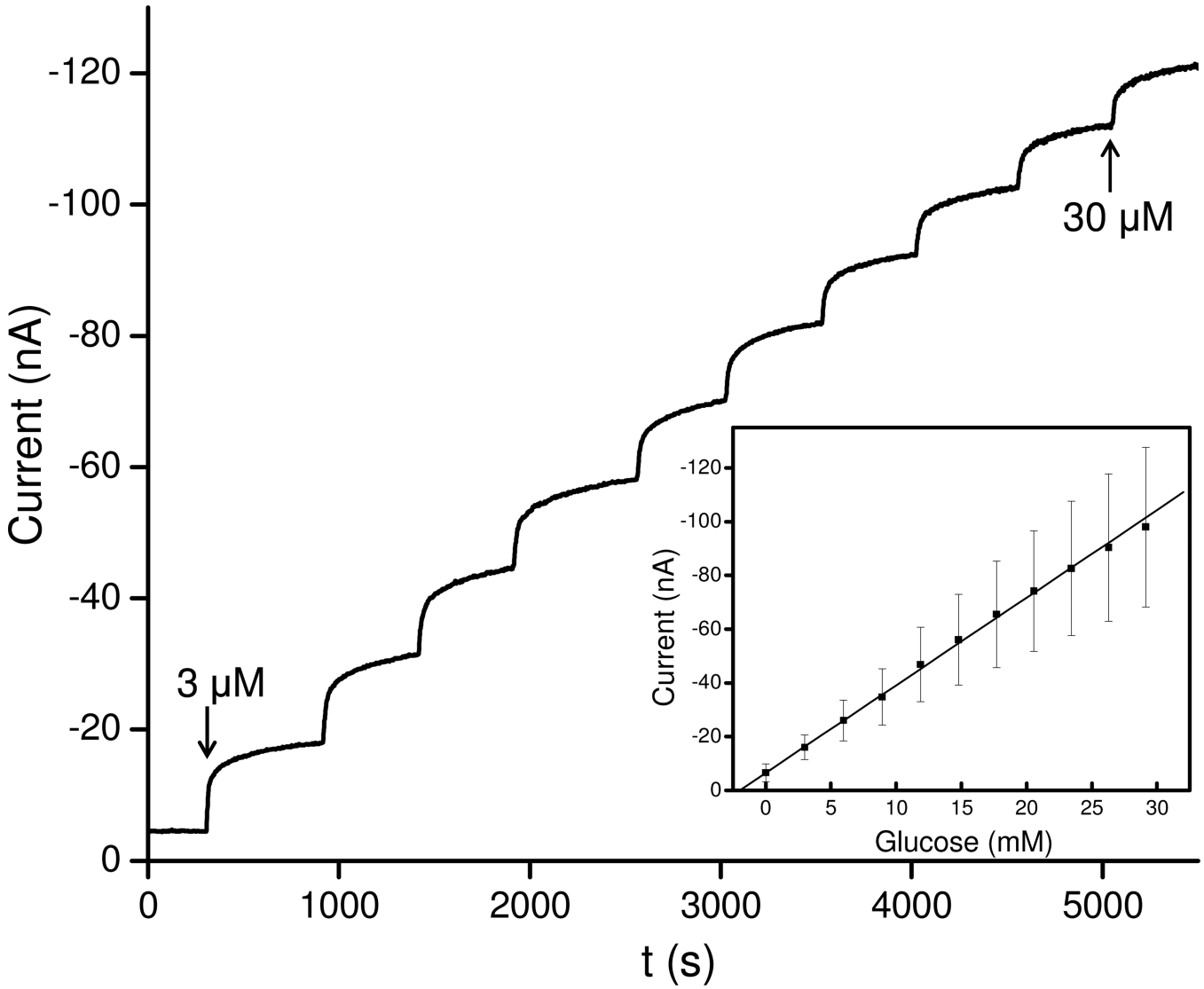

Figure 4.
Representative calibration curve for glucose biosensors coated with 15 mol% AEAP/NO-PTMOS xerogels, both real-time (main graph) and as a function of glucose concentration (inset).

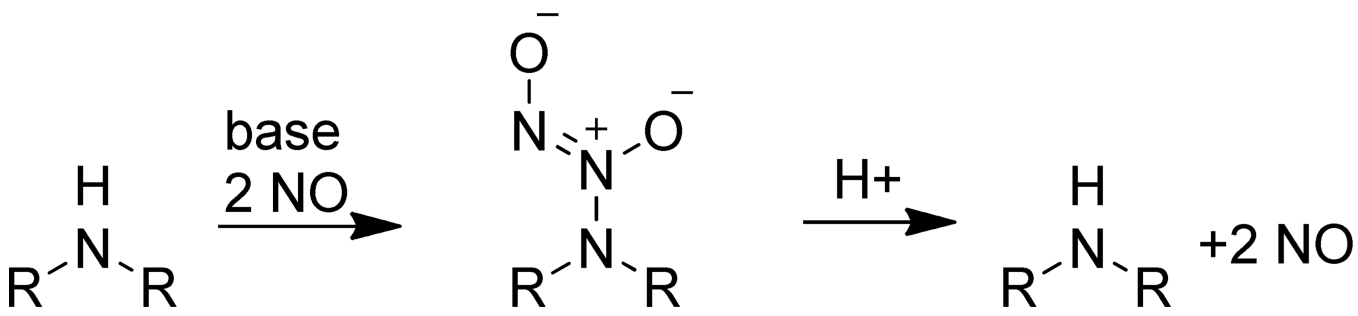

Scheme 1.
Formation of *N*-diazeniumdiolates on secondary amines and pH-dependent decomposition to produce NO.

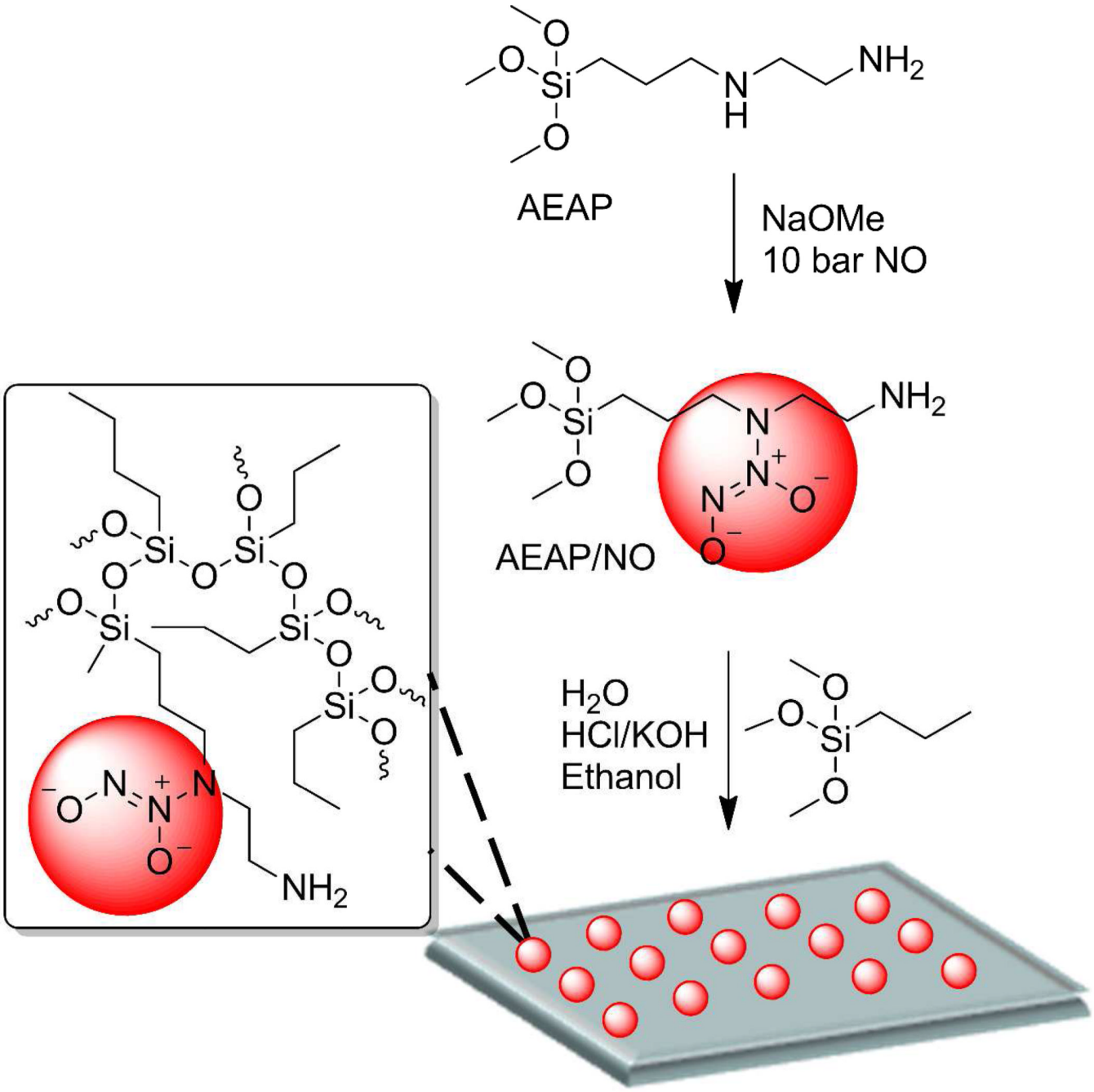

Scheme 2.

Synthesis of the “pre-diazeniumdiolated” NO-releasing xerogels. After reacting AEAP with NO to yield AEAP/NO, the *N*-diazeniumdiolated precursor is reacted with PTMOS, and cast onto an appropriate substrate. Subsequent drying/curing results in the formation of an *N*-diazeniumdiolate-modified xerogel film.

Table 1

Nitric oxide release, conversion efficiency, and spectroscopic parameters of *N*-diazeniumdiolate-modified silanes.

aminosilane	$[NO]_t$ (μmol NO μmol^{-1} silane)[a]	half-life (min)	λ_{max}(nm)	ε (mM^{-1} cm^{-1})[b]
AEAP	0.98 ± 0.17	130 ± 20	251	14.4 ± 2.5
MAP	1.47 ± 0.21	2.0 ± 0.3	249	10.0 ± 0.1
EAiB	1.38 ± 0.07	7.9 ± 1.7	249	9.5 ± 0.1

[a] Theoretical maximum of 2 mol NO per mol amine-functionalized silane

[b] Concentration of *N*-diazeniumdiolate-modified silane taken from chemiluminescent NO release totals

Table 2

Nitric oxide release from *N*-diazeniumdiolate modified xerogels.

		total NO	total NO	max flux	half-life	duration[a]
Silane	mol% silane	(μmol cm^{-2})	(μmol mg^{-1})	(pmol cm^{-2} s^{-1})	(h)	(h)
AEAP	5	0.55 ± 0.05	0.31 ± 0.03	73.8 ± 5.0	5.7 ± 0.2	29.2 ± 7.6
AEAP	10	1.75 ± 0.53	0.81 ± 0.25	193 ± 83	6.4 ± 2.1	52.4 ± 13.4
AEAP	15	2.60 ± 0.60	1.03 ± 0.24	307 ± 101	4.0 ± 0.5	41.7 ± 4.0
MAP	5	0.39 ± 0.04	0.21 ± 0.02	162 ± 71	1.7 ± 1.3	11.1 ± 0.95
MAP	10	1.41 ± 0.35	0.59 ± 0.15	262 ± 93	3.1 ± 1.3	27.7 ± 7.4
MAP	15	2.40 ± 0.51	1.00 ± 0.21	590 ± 174	1.9 ± 0.7	35.7 ± 6.4
EAiB	5	0.45 ± 0.04	0.19 ± 0.02	126 ± 8	3.8 ± 1.2	20.4 ± 1.9
EAiB	10	1.48 ± 0.09	0.62 ± 0.04	439 ± 9	2.6 ± 0.5	48.8 ± 10.5
EAiB	15	3.13 ± 0.40	1.22 ± 0.15	312 ± 142	4.2 ± 1.7	90.8 ± 22.6

[a]Time until flux drops below a threshold of 1.5 pmol cm^{-2} s^{-1}, i.e., the flux required to inhibit bacterial adhesion.

ACS Appl Mater Interfaces. Author manuscript; available in PMC 2014 June 12.

Table 3

Nitric oxide release totals and conversion efficiency from both pre- and post-diazeniumdiolated xerogels.

xerogel (15 mol%)	storage capacity[a] (%)		NO retention[b] (%)
balance PTMOS	post-diazeniumdiolated	pre-diazeniudiolated	pre-diazeniumdiolated
AEAP	0.40 ± 0.12	39.6 ± 9.1	80.7 ± 18.6
MAP	0.034 ± 0.01	41.7 ± 8.9	56.8 ± 12.1
EAiB	0.078 ± 0.03	51.6 ± 6.6	74.9 ± 9.6

[a] Percentage of *N*-diazeniumdiolates in the film compared to the total amount of secondary amines contained within

[b] Percentage of *N*-diazeniumdiolates in the film compared to the total amount of *N*-diazeniumdiolate-modified precursors added

Table 4

Properties of enzyme-based glucose biosensors coated with pre-diazeniumdiolated 15 mol% AEAP/NO-PTMOS xerogels after 0, 4 or 7 d immersion in PBS.

immersion time (d)	sensitivity (nA mM^{-1})	response time (s)	dynamic range (mM)	R^2
0	3.4 ± 0.8	530 ± 5	1–24	0.9787
4	3.3 ± 1.1	375 ± 26	1–30	0.9980
7	3.5 ± 1.3	274 ± 19	1–30	0.9992